Atmospheric Pollutant Concentrations under the Influences of Internal Gravity Wave and Sea-Land Breeze Circulations in the Mountainous Coastal Regions

Hyo Choi

Dept. of Atmospheric Sciences, Kangnung National University, Kangnung, Kangwondo, 210-702, Korea

and

Joon Choi

Research Center for Ocean Industrial Development, National Fisheries University of Pusan, Nam-Ku, Pusan 608-737, Korea

(Manuscript received 6 November 1995)

산악연안지역에서 내부중력파와 해륙풍순환 영향하의 대기오염농도

최 효

강릉대학교 대기과학과

최 준

부산수산대학교 해양산업개발연구소

1995년 11월 6일 접수

요 약

동쪽 연안지역에서 큰 경사를 갖인 산맥위를 흘러가는 종관규모의 서풍하에서 내부중력파와 같은 강한 하강폭풍이 산의 후면에서 발생되어 진다. 주간에 해양에서 내륙으로 향하는 중규모의 열적 강화에 의해 유도되는 해풍순환이 동쪽으로 향하는 내부중력파에 기인하여 연안의 앞바다까지만 국한된다. 따라서 연안해 근처의 표층풍은 외해나 내륙의 위치에서보다 상대적으로 더 약하다. 명백하게 서풍의 내부중력파순환과 해면근처에서 동풍 및 상층에서 서풍을 갖는 해풍순환과 같은 두개의 상이한 종류의 대기순환이 뚜렷하게 나타났다. 이런 상황에서 강릉시에서의 대기오염물질은 반대 방향의 두개의 상이한 순환에 의해 갇히게 되고 부유분진과 오존의 고농도가 초래되었다. 야간에 육지에서 연안해로 향하는 중규모의 육풍은 기존의 동쪽으로 향하는 하강풍과 협력

하여 연안지역에서 서풍의 더욱 강화를 유도할 수 있었다. 산쪽에서 연안해로 향하여 부는 강한 표층풍에 의해 조절되는 부유분진의 농도는 주간의 경우보다 야간에 비교적 더 높았으며, 상층대기로 부터 지표면으로 오존의 하향수송에 기인하여 오존의 농도가 주간보다 야간에 매우 높았다. 결과로 바람폭풍하의 산악연안지역에서 대기오염농도는 바람폭풍 전 · 후보다 더 높았다.

Abstract

Under the synoptic scale strong westerly winds flowing over the large steep mountains in the eastern coastal region, the strong downslope wind storms such as internal gravity waves should be generated in the lee-side of mountain. In the daytime a sea breeze circulation induced by meso-scale thermal forcing from sea toward inland confines to the offshore side of coastal sites due to the eastward internal gravity waves. Thus, surface winds near the coastal seas were relatively weaker than those in the open sea or the inland sites. Evidently, two different kinds of atmospheric circulations such as an internal gravity wave circulation with westerly wind and a sea breeze circulation with both easterly wind near the sea surface and westerly in the upper level were apparently produced. Under this situation the atmospheric pollutants at Kangnung city should be trapped by two different circulations in the opposite directions and resulted in the high concentrations of Total Suspended Particles (TSP) and ozone (O_3). At night a meso-scale land breeze from land toward the coastal sea could be associated with the existed eastward downslope wind and induced the more intensification of westerly winds in the coastal regions. The concentrations of TSP controled by the strong surface winds blowing from the mountain side toward the coastal sea were relatively higher at night than those in the daytime case and the concentrations of 0_3 due to the downward transport of ozone from the upper atmosphere toward the surface were also much higher at night than during the day. Consequently, the atmospheric pollutant concentrations in the mountainous coastal region under the downslope wind storms were higher than those after and before the occurrences of wind storms.

1. Introduction

The variation of atmospheric pollutant concentrations due to the development of internal gravity waves in Kangwondo coastal regions of Korea was investigated in the windy spring season. Near the coastal seas with high mountains, not only orographic effects such as downslope wind storms and internal gravity waves, but sea and land breeze phenomena often control coastal atmospheric circulations (Choi and Choi, 1994; Choi, et al., 1994; Choi and Choi, 1995; McPherson (1970); Plate, 1971; Raynor et al., 1979, Taylor, 1970).

In the last two decades Davies (1987), Lilly et al. (1982), Smith (1978, 1989) and WMO (1986) carried out the thoretical and numerical studies on the surface pressure drag and wave momentum flux in the mountain ranges. Durran and Klemp (1987), Klemp and Durran (1983), Peltier and Clark (1979), Satomura and Bougeault (1992), Smith (1989), and Smolarkiewicz and Rotunno (1989) made numerical simulations on orographic effects such as downslope winds, lee-side waves and upstream blocking. The further research on the dynamical effects of meso-scale mountains in the large scale numerical models of the atmosphere have been given by Boer et al. (1984), Friehe and Winant (1982), Hsu (1980, 1988) and Palmer et al. (1986).

When a synoptic scale strong westerly winds in spring prevailed in the north-eastern Asia including the Korean peninsula, the various meteorological phenomena such as downslope windstorms and hydraulic jumps were created by Taegwallyang mountain near Kangnung city in the eastern coastal region of Korea. In the mountainous coastal area where neither special upper level nor spatial observation point exist, it is a way to use numerical models in order to find out mountain effects and analyze atmsopheric pollutant concentrations such as Total Suspended Particle (TSP) and Ozone (O_3), when the downslope wind and the sea breeze process exist (Hsu, 1988; Lee, 1982; SethuRaman, 1982).

The purpose of this study is to explain the variations of atmospheric pollutant concentrations under the influence of downslope wind storms and sea-land breeze in the mountaineous coastal regions.

2. Numerical method and data analysis

The study area is located in the mountainous eastern coastal region of korea and consists of a complex terrain with forest, soil and sand in a high mountain called Whangbyung Mt. (1407m) (Choi and Choi, 1995; Choi, et al., 1995; Figs. 1 and 2). In order to investigate the variation of atmospheric pollutant concentrations due to the development of internal gravity waves in Kangwondo coastal regions from March 26 through 29, 1994, we used a non-hydrostatic grid point model with one way double-nesting technique.

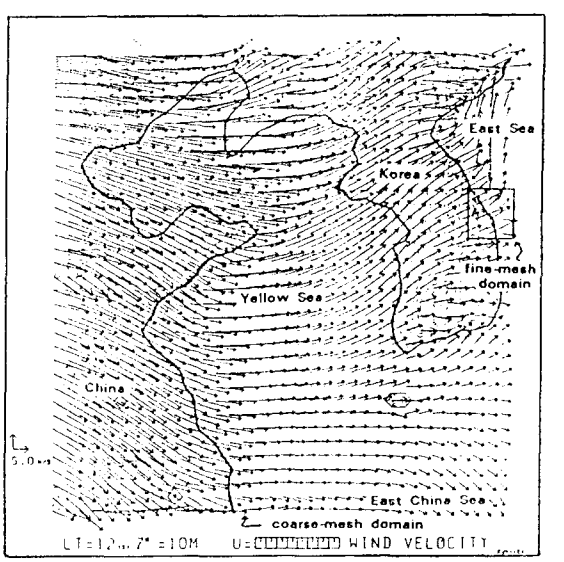

Fig. 1. Calculated surface winds (m/s) at 10m height over the ground surroung the Korean peninsula at 12 LST, March 27, 1994 in the coarse domain by using Global Analysis data.

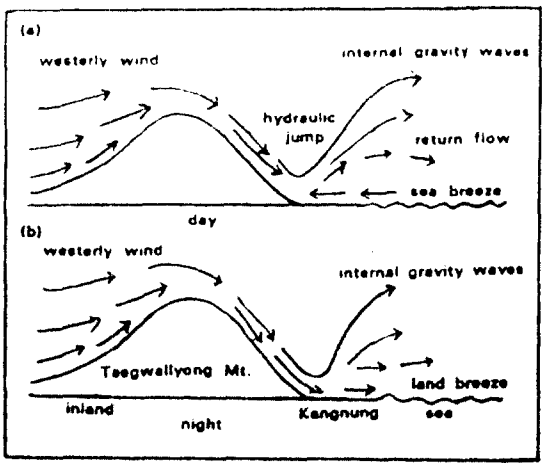

Fig. 2. Schematic profiles of winds near the mountainous coastal region for day (a) and night (b).

The horizontal resolutions of the model are 20km in the coarse-mesh model and 7km in the fine-mesh for double nesting. This model has 15 vertical levels from 10m to 6km over the ground such as 10, 45, 120, 235, 350, 500, 700, 900, 1100, 1400, 1800, 2400, 3200, 4200 and 5400m in z* coordinate called a complex terrain-following coordinate.

In the coarse-mesh model, lateral boundary data are provided with 12 hourly G-ANL (global analysis) data made by Japan Meteorological Agency (JMA). The predicted values by the coarse-mesh model were used as lateral boundary data for the fine-mesh model. Horizontal and vertical interpolations of the same global analysis data provide initial fields such as winds, potential temperature, specific humidity for all two models with different resolutions. Initial temperatures of sea surface water were obtained from sea surface temperature data acquired by NOAA (National Oceanic and Atmospheric Administration) satellite, which were analyzed by National Fisheries Research and Development Agency of Korea (NFRDA, 1994; Roll, 1965). We made a 30 hour prediction experiment from an initial field at 09 LST (Local Standard Time $=9^h+$ Greenwith Mean Time), March 27 to the next day at 12 LST, March 28 by using HITACH super computer established at Meteorological Research Institute, JMA.

Under the strong downslope storms in the mountainous coastal region, the particular regard was given to air quality analysis such as Total Suspended Particle (TSP) and Ozone (O_3). Hourly data of TSP and O_3 concentrations from 01 LST on March 26 through 24 LST on March 29 were automatically measured by SPM DUST monitor (MP 101M) and Ozone analyzer (O_3 41M) which were established at the top of Ihmdang-dong office, Kangnung and reanalyzed by Wonju Regional Environmental Administration.

3. Model formulations

3.1. Governing equations

The governing equations consist of a terrain-following coordinate system such as z*-coordinate, with the assumption of Boussinesq and anelastic approximations (Choi and Choi, 1994; Kimura, 1983; Kimura and Takahashi, 1991). The equations of motion are given by

$$\partial_t hu = fhv - h\Theta\partial_x\Pi + \Theta(z_T - z^*)\partial_x z_G \partial_z \Pi + z_T^2/h\partial_z(K_m\partial_z u) \quad (1)$$

$$\partial_t hv = -fhu - h\Theta\partial_y\Pi + \Theta(z_T - z^*)\partial_y z_G \partial_z \Pi + z_T^2/h\partial_z(K_m\partial_z v) \quad (2)$$

$$\partial_t hw^* = -z_T\Theta\partial_z\Pi + gh\theta/\Theta \quad (3)$$

$$\Pi = (P/P_{00})^{R/C_p}$$

$$\Theta = T(P_{00}/P)^{R_d/C_p}$$

where g is gravity (m/s^2) and u, v, and w* are velocity compoments in the x, y and z directions in the z* coordinate. Θ, T, z, z_T z_G and K_m imply potential temperature (K), air temperature at a given height, actual height,

height of upper boundary with its change for time and place in a model domain, height of topography and vertical diffusion coefficient for momentum (m^2/s), respectively. P, P_{00}, R, R_d and C_p are atmospheric pressure, atmospheric pressure at reference level, universal gas constant, gas constant for dry air and specific heat at constant pressure.

The first terms on the right hand side of eqs. (1) and (2) are Coriolis forces (f; Coriolis parameter, $f=2\Omega\sin\phi$, Ω; angular velocity of the earth rotation, ϕ; latitude), and the second, third and fourth terms are pressure gradient forces, adjusted terms on topography and vertical diffusion. The second and third terms of eq. (3) present vertical pressure gradient force and buoyancy, respectively. The thermodynamic equation and conservation of water vapor yield to

$$d_t h\Theta = z_T^2/h\partial_z(K_h\partial_z\Theta) + hQ_r \tag{4}$$

$$d_t hq = z_T^2/h\partial_z(K_h\partial_z q) \tag{5}$$

where Θ and q are potential temperature and specific humidity of water vapor. The second term of eq. (4) means radiative heating. In this model condensation processes are not considered. The continuity equation is given by

$$\partial_x hu + \partial_y hv + \partial_z hw^* = 0 \tag{6}$$

For the time integration of eqs. (1), (2), (4) and (5) Euler-backward scheme is adopted and for the vertical direction Crank-Nicholson scheme, respectively. z* and z are the transformed terrain-following vertical coordinate and Cartesian vertical coordinates. From eq. (1) through eq. (6) z_G and z_T are the ground surface level and top boundary level with a material surface in the model atmosphere, that is, 6000m, which can absorb gravity-wave energy generated in the lower layers. The radiation condition suggested by Klemp and Durren (1983) was adopted for the upper boundary condition. The following relations are given by

$$z^* = z_T(z - z_G)/h$$
$$h = z_T - z_G$$
$$d_t = \partial_t + u\partial_x + v\partial_y + w^*\partial_z$$
$$hw^* = z_T w + (z^* - z_T)(\partial_x z_G u + \partial_y z_G v)$$

Since horizontal scale of the phenomena is one order greater than vertical scale, eq. (3) can be converted into the following equation of hydrostatic equilibrium as

$$\partial_z \Pi = h/z_T\, g/\Theta^2\theta \tag{7}$$

In the case that the hydrostatic equilibrium can not exist, that is, non-hydrostatic state, the following pressure equation is required.

$$\begin{aligned}&\partial_{xx}\Pi + \partial_{yy}\Pi + \{(z_T/(z_T - z_G))^2 \\ &+ ((z^* - z_T)/h)^2((\partial_x z_G)^2 + (\partial_y z_G)^2)\}\partial_{zz}\Pi \\ &+ 2(z^* - z_T)/h\,\partial_x z_G\,\partial_{xz}\Pi \\ &+ 2(z^* - z_T)/h\,\partial_y z_G\,\partial_{yz}\Pi \\ &+ \{(z^* - z_T)/h(\partial_{xx}z_G + \partial_{yy}z_G) \\ &+ 2(z^* - z_T)/h^2((\partial_x z_G)^2 + (\partial_y z_G)^2)\}\partial_z\Pi \\ &= r(x,y,z^*)/(\Theta h)\end{aligned} \tag{8}$$

where r is the residual term and

$$\Pi = \pi - \pi_H$$
$$\partial_z \pi_H = gh\theta/(\Theta^2 z_T)$$
$$\begin{aligned}r(x,y,z^*) = {}&\partial_x ADVX + \partial_y ADVY + z_T/h\,\partial_z ADVZ \\ &+ 1/h\,\partial_x z_G\partial_z(z^* - z_T)ADVX \\ &+ 1/h\,\partial_y z_G\partial_z(z^* - z_T)ADVY\end{aligned} \tag{9}$$

and

$$\begin{aligned}ADVX = {}&- \partial_x huu - \partial_y huv - \partial_z huw^* + fhv \\ &- \Theta h\partial_x \pi_H - \Theta(z^* - z_T)\partial_x z_G\,\partial_z \pi_H \\ &+ z_T^2/h\partial_z(K_m\partial_z u)\end{aligned}$$
$$\begin{aligned}ADVY = {}&- \partial_x huv - \partial_y hvv - \partial_z hvw^* - fhu \\ &- \Theta h\partial_y \pi_H - \Theta(z^* - z_T)\partial_y z_G\partial_z \pi_H \\ &+ z_T^2/h\partial_z(K_m\partial_z v)\end{aligned}$$
$$ADVZ = - \partial_x huw - \partial_y hvw - \partial_z hww^*$$

The model atmosphere was vertically divided into 15 layers from 10m through 540m in the z* coordinate. The vertical diffusion coefficient was evaluated from the turbulent closure level-2 model (Mellor and Yamada; 1974). The open boundary condition developed by Oranski (1976) for u, v, θ and q was modified for the lateral boundary condition of the model

3. 2. Turbulent process

By using the turbulent closure level-2 model (Yamada, 1983) turbulent diffusion coeficients, K_m and K_h for momentum and heat of eq. (1) through eq. (5) can be expressed by

$$K_m = S_m \cdot e \cdot \ell$$
$$K_h = S_h \cdot e \cdot \ell \qquad (10)$$

where ℓ and e^2 are turbulent length determined by diagnostic approaches and turbulent kinetic energy (m^2/s^2) as

$$\ell = kz/(1 + \ell_0/kz)$$
$$\ell_0 = 0.1 \int ez\, dz / \int e dz \qquad (11)$$

and from the observation in the surface boundary layer the semi-empirical formula between S_m, S_h and flux Richardson number, R_f can be also derived as

$$S_m = 1.76\,(0.1912 - R_f)(0.2341 - R_f)/\{(1 - R_f)(0.2231 - R_f)\} = 0.085 \quad \text{for } R_f \geq 0.16$$
$$S_h = 1.318\,(0.2231 - R_f)/(0.2341 - R_f)S_m = 0.095 \quad \text{for } R_f \geq 0.16 \qquad (12)$$

where R_f can be evaluated by the function of bulk Richardson number, R_i at each grid point (Kimura, 1983) :

$$R_f = 0.6588(R_i + 0.1776 - (R_i^2 - 0.3221R_i + 0.03156)^{1/2}) \quad \text{for } R_i \leq 0.19 \qquad (13)$$
$$R_i = g/\Theta \cdot \Delta\theta \cdot \Delta z/\Delta U^2$$

Turbulent velocity, $e = (e^2)^{1/2}$ is evaluated by considering the balance between production of turbulent energy due to shear and buoancy and dissipation of turbulent energy as

$$e^2 = B_1 \ell^2 \{S_m (z_T/h)^2 \{(\partial_z u)^2 + (\partial_z v)^2\} - g/\Theta\, S_h (z_T/h)\, \partial_z \theta\} \qquad (14)$$
$$B_1 = 16.6$$

Radiation process can be explained by Katayama's radiative scheme. Considering that long wave radiations are absorbed by water vapor and carbon dioxide and flux from the ground surface toward the upper levels is regarded as positive, total net flux of long wave radiation, R_g

$$R_g = \sigma T_c^4 \tau_c + \sigma(T_{oo}^4 - T_c^4)\tau(U_{oo}) + \sum\sigma(T_i^4 - T_{i+1}^4)\tau(|U_i|)$$
$$T_c = 220K \qquad (15)$$

where σ, T_c, T_{oo} and T_i are Stefan-Boltzman's constant, critical temperature, temperature at the top of model atmosphere and temperature at the ith level, respectively. Transmission function, τ is also given by

$$\tau = \tau_{H2o} \cdot \tau_{co2}$$
$$\tau_{H2o} = (1 + 1.746U_*^{0.423})^{-1}$$
$$\tau_{co2} = 0.93 - 0.066LOG_{10}(U_{*co2})$$
$$\tau_c = (1 + 3.0U_*^{0.408})^{-1} \cdot \tau_{co2} \qquad (16)$$
$$U_* = 1/g \int q(p/p_0)^{0.6}\, dp$$
$$U_{*co2} = (p_0^2 - p^2)/p_0^2$$

where τ_{H_2O}, τ_{co2} and τ_c, U_*, q, p_O and p imply the transmission functions for H_2O, CO_2 and critical temperature (=220K), the friction velocity, specific humidity (g/cm^3), pressure (mb) at the surface and at the arbitary levels.

The absorption by water vapor due to Rayleigh scattering should be considered for the solar radiation. The solar radiation toward the earth surface, which has a positive flux and total net solar radiation at the ground yields to

$$S_g = (1-\alpha_s)\{S_{os}\,(1 - \alpha_A)/(1 - \alpha_A \alpha_s) + S_{oA}(1 - A(x))\}$$
$$S_{os} = 0.651\, S_o \cos\zeta \qquad (17)$$
$$S_{oA} = 0.349\, S_o \cos\zeta$$

where S_O is a solar constant, and S_{OS} and S_{OA} are scattering part of solar radiation ($\lambda < 0.9\mu$) and absorption one ($\lambda > 0.9\mu$). ζ is solar zenth angle, which is a function of latitude (ϕ), declination (δ) and time angle (h). α_S and α_A are albedos of atmosphere and earth surface, respectively. A (x) is an absorbing function of

solar radiation and is calculated by

$$\cos\zeta = \cos\psi\cos\delta\cosh + \sin\psi\sin\delta$$
$$\alpha_A = 0.085 - 0.247 LOG_{10}(p/p_O \sec\zeta)$$
$$A(x) = 0.273x^{0.303} \qquad (18)$$
$$x = U_{gT}\sec\zeta.$$

The heating rate of atmosphere due to solar radiation of eq. (3), Q_r can be approximated by the following Newtonian cooling due to long wave radiation.

$$Q_r = 10^{-5}(T_g - T) \quad \text{for } T > T_g \qquad (19)$$

and in the opposite case ($T > T_g$)

$$Q_r = 0 \quad \text{for } T \le T_g \qquad (20)$$

where T and T_g are air temperature and surface temperature at the ground level, respectively.

Since the physical properties such as air temperature in the surface layer have a great vertical variations, we assume the lowest level of the model to be a constant flux layer and adopt the similarity theory. For the surface energy balance momentum flux, τ, sensible heat flux, H and latent heat flux, E are written by

$$\begin{aligned} \tau/\rho &= -(u_*)^2 \\ &= -k^2|u^2|/\phi_m^2 \\ H/(C_p\rho) &= -\theta_* u_* \\ &= -k^2|u|(\theta_1 - \theta_g)/(\phi_m\phi_h) \\ E/(L\rho) &= -q_* u_* \\ &= -k^2|u|(q_1 - q_g)/(\phi_m\phi_h) \end{aligned} \qquad (21)$$

where ρ is the air density, q_* the water vapor scale, u_*, friction velocity, θ_*, the potential temperature scale, k, the Von Karman constant and the subscription 1 and g mean the lowest and ground level of the model. Businger (1973), Monin (1970), Panofsky and Dutton (1984), Paulson (1970) and Williams (1980) suggest the formula of the integrated universal functions, ϕ_m and ϕ_h as follows :

$$\phi_m = \int \Phi_m/\zeta \, d\zeta$$
$$\phi_h = \int \Phi_h/\zeta \, d\zeta \qquad (22)$$

here $\zeta = z/L$, $\zeta_O = z_o/L$ and L is Monin-Obukhov length scale defined as

$$L = \rho C_p \theta u^{*3}/kgH$$

For unstable conditions ($\zeta = z/L < 0$)

$$\phi_m = \ell_n\{(1+X^2)/2 \cdot ((1+X)/2)^2)\} - 2\arctan X + \pi/2 \qquad (23)$$

where $X(= \Phi_m^{-1}(z/L)) = (1 - 15\, z/L)^{1/4}$

For stable condition ($\zeta > 0$)

$$\phi_m = -4.7\zeta \qquad (24)$$

where $\Phi_m(\zeta) = 1 + 4.7\zeta$

For neutral condition ($L = \infty \rightarrow z/L \rightarrow 0$)

$$\Phi_m(\zeta) = 1 \qquad (25)$$

In the similar way,

For unstable condition ($\zeta < 0$)

$$\Phi_h = (1 - 15\zeta)^{-1/2} \qquad (26)$$

and for stable condition ($\zeta > 0$)

$$\Phi_h = 1 + 4.7\zeta \qquad (27)$$

where $\zeta = R_i\, \phi m^2/\phi n$

$$R_i = g/\Theta(\Theta_1 - \Theta_g)\,\Delta z_1/|u|^2$$

Deardorff (1978) suggested a force restore method for the prediction of earth surface temperature in the case of bare ground condition as

$$\partial\theta_g = (S_g - R_g - H - E)/C_1 - (\theta_g - \theta_o)/C_2 \qquad (28)$$

where θ_g and θ_O are grouns surface potential temperature and underground temperature. The coefficients, C_1 and C_2 can be evaluated by diurnal period, τ_d (= 24^h), heat capacity of

underground soil, C_g (cal/cm^3/K) and heat conductivity, kg (cal/cm/k/sec) and can be written as

$$C_1 = 0.5\ (\tau_d C_g k_g/2\pi)^{1/2}$$
$$C_2 = \tau_d/2\pi \qquad (29)$$

Assuming that evaporation coefficient, B_g at the ground is constant, specific humidity at the ground surface, q_g can be derived as

$$q_g = B_g\, q_s(T_g) + (1 - B_g)q_1 \quad \text{for } q_s(T_g) \geq q_1$$
$$q_g = q_s(T_g) \quad \text{for } q_s(T_g) < q_1 \qquad (30)$$

and now, the wetness of bare ground, w_g(= 0.2cal/cm^3/k) defined as the ratio of available water content to maximum available water content can be predicted as

$$C_g = 0.2(1 + w_g)$$
$$k_g = (0.386 + 0.15w_g)\ 10^{-2} \qquad (31)$$
$$B_g = \min(1,\ 2w_g)$$

where we treat w_g as 0.2 for the spring time (Choi and Choi, 1995).

4. Result and discussion

4.1. Wind fields

During the period of March 26 through 28, 1994 synoptic-scale strong westerly winds were blowing over the north-eastern Asian counties, especially China, Korea and Japan. On March 26 the surface winds were moderate, but as shown in Figs. 1 and 3-a, at 12 LST on March 27, 1994 the westerly winds penetrate into the Korean peninsula, passing by the eastern coastal mountain regions and producing strongly enforced local atmospheric

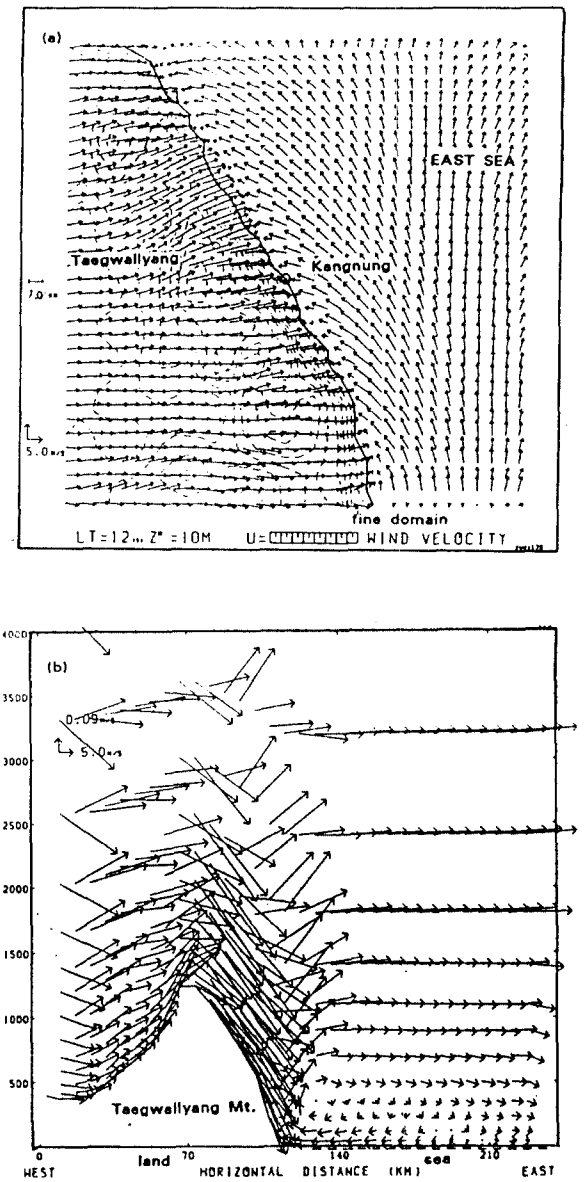

Fig. 3. Surface winds(m/s) at 10m height over topography(dot line) near kangnung area of Korea (a) and vertical profiles of winds(m/s) on 15-levels over the straight cutting line from Kangnung near to Taegwallyang Mt. at 12 LST, March 27, 1994 (b).

Fig. 3-b show the vertical profiles of wind speeds on 15 levels over the straight cutting line from Kangnung (east) to Whangbyung Mountain (west) in the model domain. As the

synoptic scale westerly winds in the eastern coastal region with the large steep mountains rapidly flow over the mountains, they could be the strong downslope winds such as internal gravity waves, which should be generated in the lee-side of mountain and coastal seas. Hence, from the vertical profiles of horizontal winds at each level of 15 levels the downslope winds showed hydraulic jumps with bounding foreward, and they could be wind storms which blew toward the eastern coastal sea.

During the day a sea breeze circulation induced by meso-scale temperature gradient of air takes a place from sea toward inland sites, but the stretch of a sea breeze circulation toward inland confines to just coastal site due to the entries of eastward internal gravity waves. Thus, surface winds near the coastal seas were relatively weaker than those in the open sea or inland (Fig. 3-a). Consequently, we could observe two different kinds of atmospheric circulations (two cells) which were an internal gravity wave circulation with westerly wind and a sea breeze circulation with both easterly wind near the sea surface and westerly in the upper level such as a circular flow pattern (Figs. 2 and 3-b).

Near the sunset time at 18 LST the wind pattern was similar to that at 12 LST, but the sea breeze circulation became shallower and shallower with weak wind speeds (Figs. 4-a and 4-b). After this time, the westerly downslope winds, which could be associated with land breeze blowing from inland toward sea were intensified by momentum transfer from the strong upper level winds toward the surface and thus, the surface winds near the Kangnung city became stronger and stronger before sunrise (Figs. 5-a and 5-b). At 06 LST on the next day morning, that is, sunrise time as the center of the wind storm was located in the lower level near the surface, the surface winds induced by the strong downslope winds were still westerly, even if sea breeze with a relative weak wind speeds started (Figs. 6-a and 6-b).

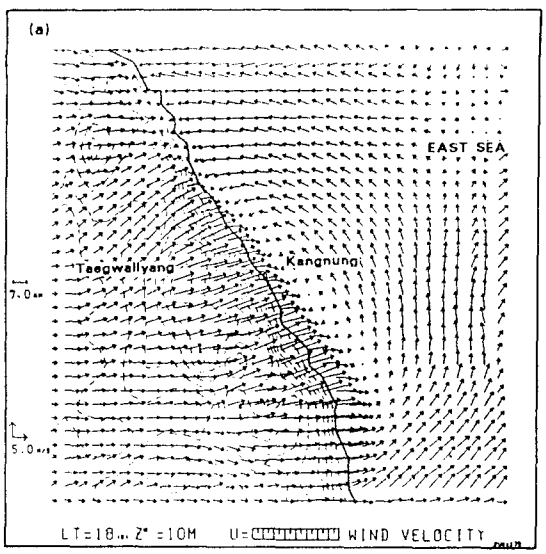

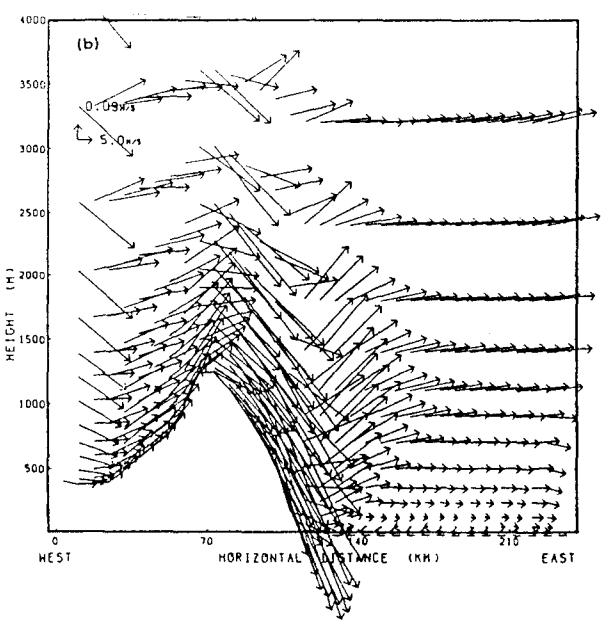

Fig. 4. As shown in Fig. 3. except for 18 LST, March 27, 1994

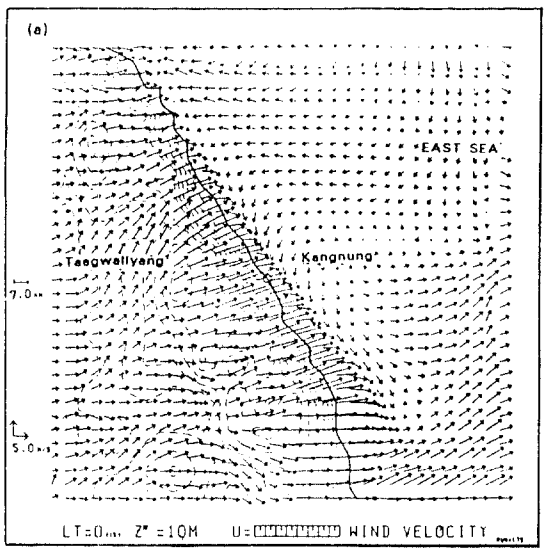

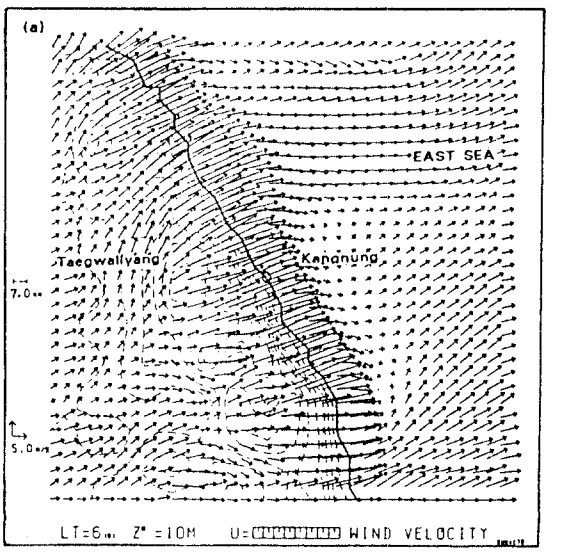

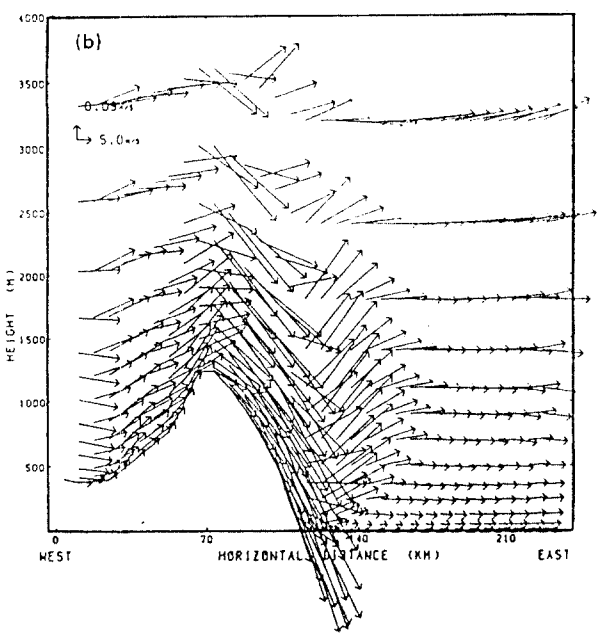

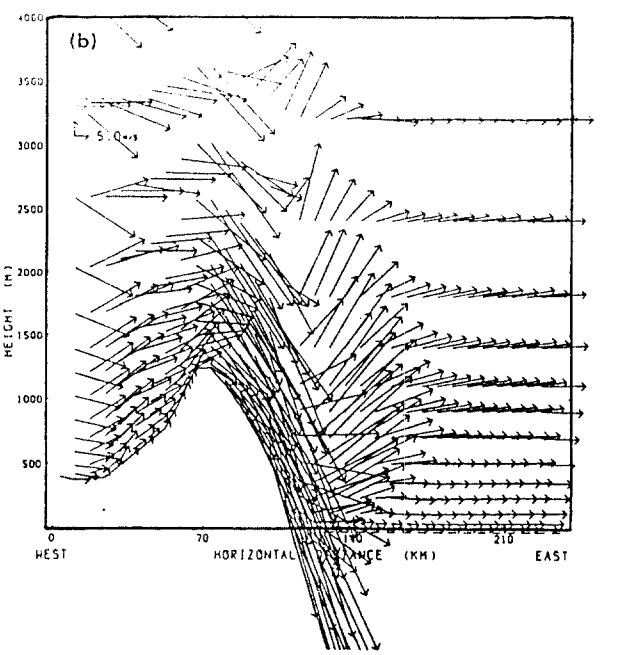

Fig. 5. As shown in Fig. 3. except for 00 LST, March 28, 1994.

Fig. 6. As shown in Fig. 3. except for 06 LST, March 28, 1994.

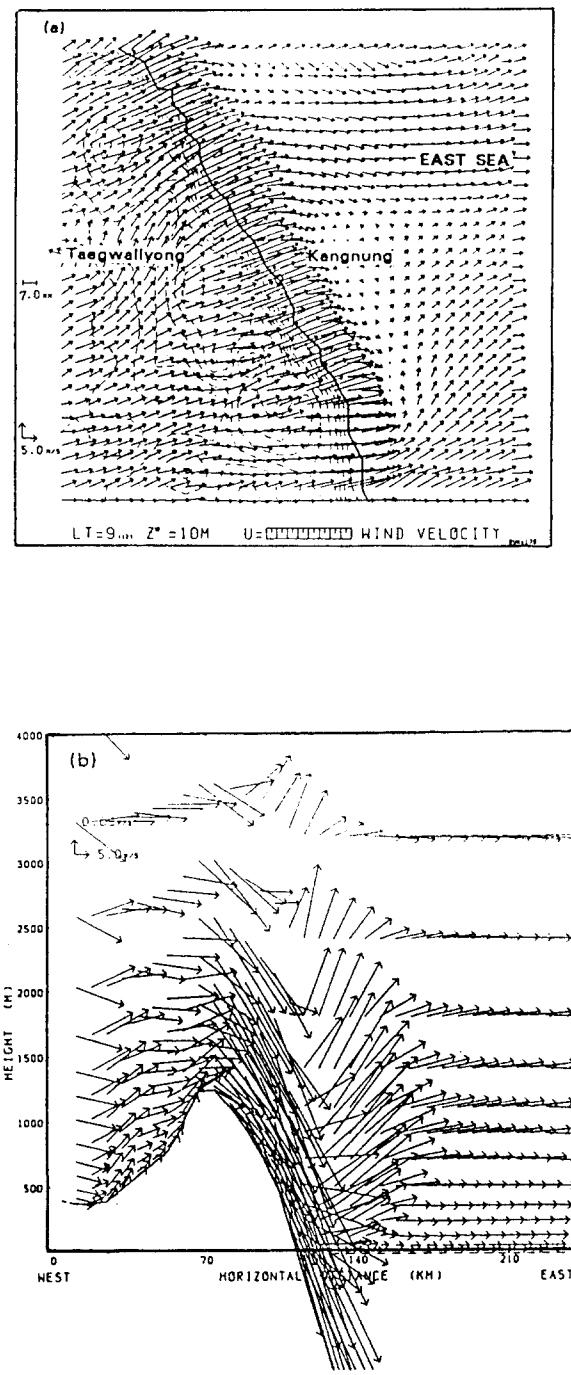

Fig. 7. As shown in Fig. 3. except for 09 LST, March 28, 1994.

At 09 LST the center of the wind storm was observed at the almost same position and the strong westerly winds could suppress the easterly sea breeze, showing the resultant westerly surface winds near Kangnung city (Figs. 7-a and 7-b). During the day on March 28 the wind patterns were very similar to those on March 27. On March 29 there was no downslope wind storms occurred in the lee side of Taegwallyang mountain and the surface winds at Kangnung were weak.

4.2. Concentrations of Atmospheric pollutants

Figs. 8-a and 8-b depicted the hourly variations of atmospheric pollutant concentrations such as Total Suspended Particle (TSP; g/m^3) and Ozone (O_3; ppb) at Kangnung environmental observation point from March 26 through 29, 1994, during the periods of the strong synoptic scale westerly winds as mentioned above.

From 01 LST to 16 LST on March 26 the concentrations of TSP at Kangnung city were in the range of 12.3 $\mu g/m^3$ to 23.3 $\mu g/m^3$. After this time their concentrations tend to be higher until 22 LST and became lower again. The hourly variations of TSP concentrations on March 27 showed a similar pattern with a little bit higher concentrations than those of March 26, and the range of concentrations were from 14.3 $\mu g/m^3$ t0 40.7 $\mu g/m^3$.

For instance, at 15 LST on March 27 under the existance of two kinds of atmospheric circulations such as an internal gravity wave circulation with westerly wind, that is, eastward downslope wind storms and a sea breeze circulation with both easterly wind near the sea surface and westerly in the upper level, the atmospheric pollutants at Kangnung city should be trapped by the two circulations in the opposite directions. At this time the horizontal wind speed of the downslope wind near the coastal surface reduced by the westward stretch of sea breeze was relatively weak with the speed of 2.0m/s and the concentration of

TSP around this time (16 LST) has a very high magnitude of 40.7 $\mu g/m^3$ (Figs. 3-b and 8-a). Since two kinds of atmospheric circulations existed in the Kangnung coastal region from 15 LST on March 27 until 21 LST, the concentrations of TSP still have high magnitudes of 31.7 $\mu g/m^3$ to 40.0 $\mu g/m^3$.

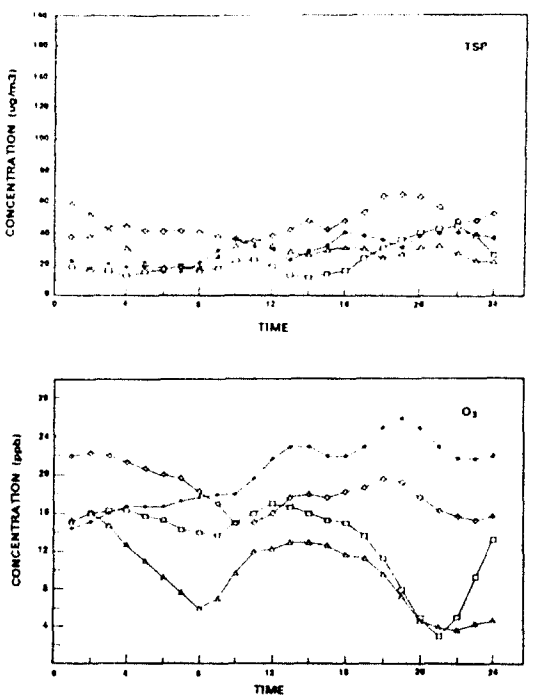

Fig. 8. Hourly concentrations of Total Suspended Particle (TSP : $\mu g/m^3$) (a) and Ozone (O_3:ppb) at Kangnung environmental observation point. □, ●, ◇, △ mean March 26, 27, 28 and 29, 1994.

However, at 00 LST March 28 the association of the eastward downslope wind storm due to the intensification of synoptic scale westerly winds with a meso-scale land breeze from land toward the coastal sea could make one atmospheric circulation in the coastal region, and the suspended particles were not trapped due to eastward land breeze, but moved toward the coastal seas. The concentration of TSP at 00 LST March 28 was 36.3 g/m^3, which was 3.7 g/m^3 lower than that of 21 LST March 27 in the trap situation and the surface wind speed near Kangnung city was 5 m/s.

As the nighttime went on, the downslope wind storms coild be more intensified by both momentum transfer from the strong upper level winds toward the surface and land breeze, and the surface winds near the Kangnung city became strong. Under the strong surface winds a large amount of dusts could fly over the ground. For the nighttime hours from 01 LST on March 28 through 09 LST their concentrations became in the higher range of 37.3 $\mu g/m^3$ to 44.0 $\mu g/m^3$.

During the daytime after 09 LST March 28 two kinds of circulations, especially under the strong development of downslope winds should be produced again with the surface wind speed of 18 m/s at Kangnung city, and the high concentrations of TSP with a maximum value of 64.7 $\mu g/m^3$ could remain until 18 LST. There were some changes of TSP concentrations from 19 LST on March 28 to 03 LST on March 29. After this time there was no strong downslope wind and the typical pattern on the daily variation of TSP concentrations occurred from 04 LST to 24 LST on March 29.

The hourly distributions of ozone concentrations from March 26 through 29 were shown in Fig. 8-b. During the observation period of strong downslope wind storms from March 27 through 28, the high concentrations of ozone were detected in the range of 14.3 ppb to 26.0 ppb on 27 and 15.0 ppb to 22.3 ppb on 28 at Kangnung city in the coastal region and the hourly distributions of ozone concentrations described a similar pattern each other. The concentrations of ozone for this period were lower during the day than at

night, and their maximum concentrations of 26 ppb on March 27 and 22.3 ppb on March 28 were observed in the nighttime hours after sunset, especially at 19 LST and 02 LST, respectively. Because for the nighttime hours on March 27 and 28 land breeze from the inland toward the coastal sea could be associated with the existed eastward downslope wind and the downslope wind storms could be more intensified at night than during the day in the lee side of Taegwallyang mountain of the coastal region such as Kangnung city (Figs. 4-b and 5-b). Under this situation momentum could be transported from the strong upper level winds toward the earth surface and the transfer of some amounts of ozone may simultaneously occur from the upper layer toward the surface, resulting in their maximum concentrations of O_3 at night.

In the case of no downslope winds on March 26 and 29, the relatively lower concentrations of ozone were measured in the range of 8 ppb to 16.7 ppb on 26th with a maximum value at 12 LST and 3.7 ppb to 16 ppb on 29th with a maximum at 13 LST, showing a similar pattern on their two hourly distributions. On March 26 and March 29 a typical pattern of ozone concentration, which showed the maximum concentration in the afternoon, was detected.

It has been known that the ozone concentration at the inland city generally is higher during the day than at night, due to the photochemical reaction of NOx by solar radiation. The high ozone concentrations near the surface at the coastal city, Kangnung for the daytime hours may be partly affected by the inland movement of ozone over the coastal sea, because the sea breeze with easterly winds extended to Kangnung until sunset. Thus, during the day the ozone concentrations at Kangnung would be controled by the photochemical reaction and the transfer of ozone from coastal sea, but at night neither photochemical reaction nor sea breeze existed, resulting in the lower concentration of ozone than those of daytime.

When the downslope winds were strongly developed, the concentrations of atmospheric pollutants in the case of one atmospheric circulation from the mountain side toward the coastal sea at night were relatively higher than those in the two different kinds of circulations during the day. As result, we may explain that the hourly variations of ozone concentrations had, in part, the similar hourly variations of Total Suspended Particle concentrations.

5. Conclusion

As the strong synoptic scale westerly winds rapidly flow over the large steep mountains in the eastern coastal region, the downslope wind storms downslope winds such as internal gravity waves should be generated in the lee-side of mountain and the downslope winds result in hydraulic jumps with bounding eastward.

In the daytime a sea breeze circulation induced by meso-scale temperature gradient of air takes a place, but a sea breeze circulation toward inland confines to the offshore side of coastal seas due to the eastward internal gravity waves. Thus, surface winds near the coastal seas were relatively weaker than those in the open sea or inland. We could observe two different kinds of atmospheric circulations (two cells) which were an internal gravity wave circulation with westerly wind and a sea breeze circulation with both easterly wind near the sea surface and westerly in the upper level. Under this situation suspended particles (dust) and ozone at Kangnung city should be

trapped by the two different circulations in the opposite directions and the concentration of TSP around this time has a very high magnitude.

On the other hand, at night under the intensification of westerly downslope wind storms associated with land breeze, the surface winds became stronger and the suspended particles could easily fly over the ground surface. The concentrations of TSP at night were relatively higher than those in the two different circulations during the day. The ozone concentrations in the nighttime hours were also higher than those during the day, becase the ozone should be transported from the upper atmosphere toward the surface due to the momentum transfer from the strong upper level wind speeds. However, without the wind storms the surface wind speeds were not high enough to produce a lot of flying dusts and TSP concentrations without storms should be much lower than those with storms. In this case, the ozone concentrations show a typical pattern, which has a maximum value of ozone near midday and their low values at night.

Consequently, when the downslope winds were strongly developed, the surface wind speeds at Kangnung also became larger, resulting in the high concentrations of atmospheric pollutants.

Acknowledgement

The author would like to express their thanks to Meteorological Research Institute, Japan Meteorological Agency and National Fisheries Research and Development Agency for the meteorological and oceanic data. This paper was supported in part by NON DIRECTED RESEARCH FUND, Korea Research Foundation, the Ministry of Education in 1995, under grant for "Variation of atmospheric pollution concentrations due to the development of internal gravity waves in Kangwondo coastal regions" (이 論文은 "江源道 東海沿岸에서 內部重力波의 發達에 依한 大氣汚染 濃度 變化"에 對한 1995年度 敎育部 韓國學術振興 財團의 自由公募課題 硏究費에 依하여 硏究되었 음).

References

Boer, G. J., N. A. McFarlane, and R. Laprise, The climatology of Canadian climate center general circulation model as obtained from a five-year simulation, Atmos. Ocean, 22, 430~473, 1984.

Businger, J. A., Turbulence transfer in the atmospheric surface layer, In "Workshop on Micrometeorology" ed. by D. A. Haugen, Amer. Meteor. Soc., 67~100, 1973.

Choi, H. and J. Choi, Characteristics of onshore winds in the coastal thermal internal boundary layer, J. Korean Meteor. Soc., 30, 1~11, 1994.

Choi, H., T. Yoshikawa, S. Takahashi, J. Choi and Y. Moon, Numerical modelling on the growth of recession of thermal internal boundary layers in the Cheju coastal region of Korea, J. East. Coast. Res., 5, 11~38, 1994.

Choi, H., Three dimensional numerical modelling on the growth of thermal internal boundary layers in the Cheju coastal region of Korea, J. Korean Meteor. Soc., 31 in press, 1995.

Choi, H. and J. Choi, Numerical modelling for atmospheric and oceanic circulations in the eastern coastal seas of Korea, submitted to Lar Mer, 1995.

Choi, H., J. Choi, S. Takahashi and T. Yoshikawa, Numerical modelling of coastal fogs under the influence of East Korea Warm Current and coastal mountains, Oral presentation in the 8th Pacific Marginal Sea and Japan-East China Sea Workshop, Masuyama, Japan, 1995.

Choi, H. and J. Choi, Variation of atmospheric pollutant concentrations under the influence of windstorms in the lee side of coastal mountains, 1st International Joint Seminar on Regional Deposition Processes in the Atmosphere, 207~238, Seoul, Korea, 1995.

Davis, H. C., Observational studies and interpretation of the mountain pressure drag during ALPEX, in observation, theory and modelling of orographic effects, ECMWF, Reading, 113, 136, 1987.

Durran, D. R. and J. B. Klemp, Another look at downslope wind storms, Part II : Non linear amplication beneath wave overturning layers, J. Atmos. Sci, 44, 3402~3412, 1987.

Deardoff, J. W., Efficient prediction of ground surface temperature and moisture with inclusion of a layer of vegetation, J. Geophys. Res., 38, 659~661, 1978.

Friehe, C. A. and C. D. Winant, Observation of wind and sea surface temperature structure off of the northern California coast, 1st International Conference on Meteorology and Air/Sea Interaction of the Coastal Zone, Hague, Amer. Meteor. Soc., 209~214, 1982.

Hsu, S. A., Research in the coastal meteorology : basic and applied, 2nd Conference on Coastal Meteorology, Los Angles, Amer. Meteor. Soc., 1~7, 1980.

Hsu, S. A., Coastal Meteorology, Academic Press. pp. 260 1988.

Kimura, F., A numerical simulation of local winds and photochemical air pollution (I) : two-dimensional land and sea breeze, J. Meteor. Soc. Japan, 61, 862~878, 1983.

Kimura, F. and S. Takahashi, The effects of land-use and anthropogenic heating on the surface temperature in the Tokyo metropolitan area : numerical experiment, Atmos. Environ., 25, 155~164, 1991.

Klemp, J. B. and D. R. Durran, An upper condition permitting internal gravity wave radiation in numerical mesoscale models, Mon. Wea. Rev., 111, 430~440, 1983.

Lee, Y., The prediction of thermal internal boundary layer growth and fumigation, 1st International Conference on Mteteorology and Air/Sea Interaction of the Coastal Zone, Hague, Amer. Meteor. Soc., 83~86, 1982.

Lilly, D. K., J. M. Nicholls, R. M. Chervin, P. J. Kennedy and J. B. Klemp, Aircraft measurements of wave momentum flux over the Colorado Rocky Mountains, Q. J. R. Meteor. Soc., 108, 625~642, 1982.

Mellor, G. L. and T. Yamada, A hierachy of turbulence closure models of planetary boundary layers, J. Atmos. Sci., 31, 1791~1805, 1974.

NFRDA, Analyzed NOAA satellite picture on the sea surface temepratures in the East Sea (Japan Sea), National Fisheries Research and Development Agency, 1994.

Orlanski, I., A simple boundary condition for unbounded hyperbolic flows, J. Comp. Phys., 21, 251~269, 1976.

Palmer, T. N., G. J. Smith and R. Swinbank, Alleviation of a systematic westerly bias in general circulation and NWP models through and orographic gravity wave drag parameterization, Q. J.

R. Meteor. Soc., 112, 1001~1039, 1986.

Paulson, C. A., The mathematical representation of wind speed and temperature profiles in the unstable atmospheric surface layer, J. App. Meteor., 9, 857~861, 1970.

Peltier, W. R. and T. L. Clark, The evolution and stability of finite amplitude mountain waves, Part II : Surface wave drag and severe downslope windstorms, J. Atmos. Sci., 36, 1498~1529, 1979.

Plate, E. J., Aerodynamic characteristics of atmospheric boundary layers, U.S. Atmospheric Energy Commission, pp. 190, 1971.

Raynor, G. S., S. SethRaman and R. M. Brown, Formation and characteristics of coastal internal boundary layer during onshore flows, Boundary Layer Meteor., 16, 487~514, 1979.

Roll, H. V., Physics of the marine atmosphere, Academic press, New York, pp. 426, 1965.

Satomura, T. and P. Bougeault, Orographic wave drag during PYREX experiment, in Spring Meeting of the Meteorological Society of Japan, Tsukuba, pp. 282, 1992.

SethuRaman, S., Observation of the bounadry layer wind structure near land-sea interface, 1st International Conference on Meteorology and Air/Sea Interaction of the Coastal Zone, Hague, Amer. Meteor. Soc., 4~7, 1982.1

Smith, R. B., A measurement of mountain drag, J. Atmos. Sci., 35, 1644~1654, 1978.

Smith, R. B., Hydrostatic airflow over mountains, Adv. Geophys., 31, 1~41, 1989.

Smolarkiewicz, P. K. and R. Rotunno, Low Froude number flow past three dimensional obstacles, Part I : Baroclinically generated lee vorties, J. Atmos. Sci., 46, 1154~1164, 1989.

Taylor, P. A., A model of airflow above changes in surface heat flux, temperature and roughness for neutral and unstable conditions, Boundary Layer Meteor., 1, 18~39, 1970.

Williams, R. G., A procedure for wind field construction from measured data which utilizes local surface roughness, 2nd Conference on Coastal Meteorology, Los Angles, Amer. Meteor. Soc., pp. 307, 1980.

WMO, Scientific results of the Alpine experiment, GARP publication series, 27, WMO, Geneva, 1986.

Yamada, T., Simulation of nocturnal drainage flows by a q2-l turbulence closure model, J. Atmos. Sci., 40, 91~106, 1983.